MODELING AND STEADY-STATE PERFORMANCE ANALYSIS OF A BRUSHLESS DOUBLY FED TWIN STATOR INDUCTION GENERATOR

Duro Basic[1], Jian Guo Zhu[2], and Gerard Boardman[2]

[1] PDL Electronics, 81 Austin Street, Onekawa
PO Box 741, Napier, New Zealand
Phone: +64-6-843-5855 (Ext. 7154)
Fax: +64-6-843-0603
Email: duro.basic@pdl.co.nz

[2] Faculty of Engineering, University of Technology, Sydney
PO Box 123 Broadway NSW 2007, Australia
Phone: +61 2 9514 2318
Fax: +61 2 9514 2435
Email: joe@eng.uts.edu.au

Abstract

This paper presents an improved steady-state model and performance study of a brushless doubly fed twin stator induction generator (BDFTSIG). The proposed steady-state model is modified to take into account magnetic saturation and stator and rotor core loses. These modifications are essential for realistic results in the BDFTSIG applications as the control stator machine works at variable flux levels and can easily come into magnetic saturation while the rotor frequency is normally much higher than that in standard induction machines so that rotor core losses cannot be neglected. The model is verified by experiments and the performance analysis indicates the feasibility of the BDFTSIG for variable speed generator applications.

1. INTRODUCTION

Doubly fed induction machines have a great advantage in high power variable-speed generator applications as independent control of active and reactive power can be achieved by using a power electronic converter connected to the rotor circuit so that it handles only the slip power and consequently can be rated for a fraction of the stator VA rating [1,2]. To combine this great advantage of doubly fed generators with high reliability and low maintenance requirements by avoiding the use of the slip rings and brushes a renewed research effort has been made to develop alternatives for classical slip-ring doubly-fed induction machines. For example, the use of two cascaded induction machines and associated control strategies are investigated by Hopfensperger [3,4] while the control of two cascaded machines unified in one with a special rotor cage design is extensively examined by the research group at the Oregon State University [5].

In this paper we will focus our attention on so called the Brush-less Doubly Fed Twin Stator Induction Generator (BDFTSIG). Basically the BDFTSIG consists of two cascaded induction machines, magnetically and electrically insulated, with common shaft and interconnected rotors placed in a common housing. The first stator winding (power winding) is directly connected to the power system grid while the second stator winding (power winding) is supplied from a controlled voltage or current source of variable frequency. In our study a functional equivalent of the BDFTSIG comprising of two wound rotor induction machines (Fig. 1, power and control machine) is used with the rotors mechanically and electrically coupled through the slip-rings & brushes similarly as in [3,4]. The slip rings and brush gears not needed in real BDFTSIG system.

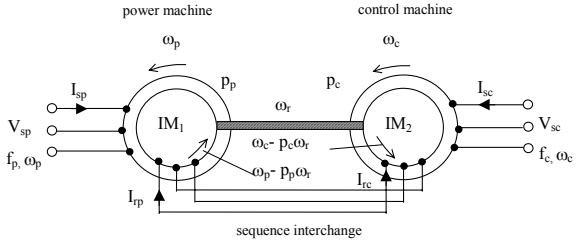

Figure 1. BDFTSIG concept.

In a special operation mode (synchronous mode) the rotor current frequency in the both machines is the same so that the power winding can be controlled through the rotors from the control stator in a brush-less manner. BDFTSIG is able to generate the power at the power system side at constant (power system) frequency and variable rotor speeds providing that the control side is fed by an appropriate frequency so that the synchronous operation is maintained. By adjusting the phase and magnitude of the control machine stator current (excitation current) the amount of the active and reactive power flowing through the power system can be dynamically controlled. For this a vector control scheme with orientation on the power machine stator flux is favourable [3] which is basically the same as the schemes in [1,2] used for standard doubly fed slip ring machines.

Major area for the application of the BDFTSIGs is considered to be high power wind generators where variable-speed operation, high reliability and low maintenance of the generators placed on high towers are very important. As all variable-speed constant-frequency generators the BDFTSIG can be controlled to maximise the system efficiency by capturing maximum wind power at the rotor speed tuned according to the wind speed (maximal power tracking), mitigate mechanical stresses on the shaft and gears caused by wind gusts (i.e. to store wind energy in the mechanical inertia of the turbine), compensate for power pulsation caused by back pressure of the tower or to adjust the generator power factor [2].

Most recently published papers have investigated the control aspects of the brush-less machines [3-5] while steady-state performance analysis have not been discussed in detail. Our goal in this paper is to present a simple steady-state model of the BDFTSIG which includes magnetic core saturation and stator and rotor core loses into account to be used for the evaluations of the BDFTSIG steady state performance, particularly the generator efficiency. Such a model is important for the BDFTSIG because the control stator is normally fed from a controlled current source so that the flux level in the control machine can vary considerably. Also, as the rotor frequency is normally much higher than that in standard induction machines, rotor core losses must be included into model. Steady state performance of a laboratory BDFTSIG set-up is evaluated by using this model and analysed. The experimental results presented compare very well with the theoretical and simulation results and confirm the effectiveness of the BDFTSIG model. Overall steady-state performance suggest that the use of the BDFTSIG for variable speed generator applications is feasible.

2. DYNAMIC MODEL

As the BDFTSIG consists of two separate induction machines connected electrically and mechanically, its model can be readily developed by combining two of the well known models of an induction machine (power and control machines). The voltage equations for power machine (p stands for power, r for rotor and s for stator):

$$\begin{aligned}\mathbf{v}_{sp} &= \left(R_{sp} + \left(s + j\, p_p \omega_r\right)L_{sp}\right)\mathbf{i}_{sp} + \left(s + j\, p_c \omega_r\right)L_{mp}\,\mathbf{i}_{rp} \\ \mathbf{v}_{rp} &= s\, L_{mp}\,\mathbf{i}_{sp} + \left(R_{rp} + s\, L_{rp}\right)\mathbf{i}_{rp}\end{aligned} \tag{1}$$

The voltage equations for control machine (c stands for control):

$$\begin{aligned}\mathbf{v}_{sc} &= \left(R_{sc} + \left(s + j\, p_c \omega_r\right)L_{sc}\right)\mathbf{i}_{sc} + \left(s + j\, p_c \omega_r\right)L_{mc}\,\mathbf{i}_{rc} \\ \mathbf{v}_{rc} &= s\, L_{mc}\,\mathbf{i}_{sc} + \left(R_{rc} + s\, L_{rc}\right)\mathbf{i}_{rc}\end{aligned} \tag{2}$$

The torque equations are:

$$\begin{aligned}T_{ep} &= \frac{3}{2}\, p_p\, L_{mp}\, imag\left(\mathbf{i}_{sp}\,\mathbf{i}_{rp}{}^{*}\right) \\ T_{ec} &= \frac{3}{2}\, p_c\, L_{mc}\, imag\left(\mathbf{i}_{sc}\,\mathbf{i}_{rc}{}^{*}\right)\end{aligned} \tag{3}$$

where all space vectors are transformed into rotor coordinates (p_p and p_c are numbers of the power and control machine pole pairs). The two rotor are mechanically connected and their windings are electrically interconnected so that the rotor currents have opposite sequence. With a such rotor interconnection, the rotor voltage and current equations can be linked by using the following identities (it is also possible to use a back-back connection without the change in the phase sequence [2]):

$$\mathbf{v}_{rp} = \mathbf{v}_{rc}{}^{*} \text{ and } \mathbf{i}_{rp} = -\,\mathbf{i}_{rc}{}^{*} \tag{4}$$

where * stands for conjugation. Finally, from Eqs. 1-4 the following model of the BDFTSIG can be derived:

$$\begin{aligned}\mathbf{v}_{sp} &= \left(R_{sp} + \left(s + j\, p_p \omega_r\right)L_{sp}\right)\mathbf{i}_{sp} + \left(s + j\, p_c \omega_r\right)L_{mp}\,\mathbf{i}_r \\ 0 &= s\, L_{mp}\,\mathbf{i}_{sp} + \left(R_{rp} + R_{rc} + s\left(L_{rp} + L_{rc}\right)\right)\mathbf{i}_r - s\, L_{mc}\,\mathbf{i}_{sc}{}^{*} \\ \mathbf{v}_{sc} &= \left(R_{sc} + \left(s + j\, p_c \omega_r\right)L_{sc}\right)\mathbf{i}_{sc} - \left(s + j\, p_c \omega_r\right)L_{mc}\,\mathbf{i}_r{}^{*}\end{aligned} \tag{5}$$

with the total torque:

$$\begin{aligned}T_e = T_{ep} + T_{ec} = \frac{3}{2}\, p_p\, L_{mp}\, imag\left(\mathbf{i}_{sp}\,\mathbf{i}_r{}^{*}\right) - \\ - \frac{3}{2}\, p_c\, L_{mc}\, imag\left(\mathbf{i}_{sc}\,\mathbf{i}_r\right)\end{aligned} \tag{6}$$

3. STEADY STATE MODEL

For the steady state analysis we will suppose sinusoidal balanced excitations at the both stators. With sinusoidal balanced supplies at the both stators the space vectors have constant magnitudes and they rotate at the corresponding slip frequencies in the rotor reference frame. For example, in the case of the stator voltages, we have:

$$\begin{aligned}\mathbf{v}_{sp} &= \sqrt{2}\, V_{sp}\, e^{j\left(\left(\omega_p - p_p \omega_r\right)t + \phi_p\right)} = \\ &= \sqrt{2}\, V_{sp}\, e^{j\phi_p}\, e^{j\left(\omega_p - p_p \omega_r\right)t} = \sqrt{2}\,\mathbf{V}_{sp}\, e^{j\left(\omega_p - p_p \omega_r\right)t} \\ \mathbf{v}_{sc} &= \sqrt{2}\, V_{sc}\, e^{j\left(\left(\omega_c - p_c \omega_r\right)t + \phi_c\right)} = \\ &= \sqrt{2}\, V_{sc}\, e^{j\phi_c}\, e^{j\left(\omega_c - p_c \omega_r\right)t} = \sqrt{2}\,\mathbf{V}_{sc}\, e^{j\left(\omega_c - p_c \omega_r\right)t}\end{aligned} \tag{7}$$

Synchronous operation can occur if the both stator excitations produce the same rotor frequency and sequence. Taking into account that the two rotors are mutually connected with interchanged phases (Eq. 4), the following equation must be satisfied to obtain the synchronous operation:

$$\begin{aligned}e^{j\left(\omega_p - p_p \omega_r\right)t} &= e^{-j\left(\omega_c - p_c \omega_r\right)t} \\ \omega_p - p_p\, \omega_r &= -\left(\omega_c - p_c \omega_r\right)\end{aligned} \tag{8}$$

so that the synchronous speed is given by:

$$\omega_{synch} = \frac{\omega_p + \omega_c}{p_p + p_c} \tag{9}$$

In the synchronous mode the general dynamic model given by Eqs. 5 and 6 can be transformed into the following steady state model:

$$\begin{aligned}\mathbf{V}_{sp} &= \left(R_{sp} + j\, X_{sp}\right)\mathbf{I}_{sp} + j\, X_{mp}\,\mathbf{I}_r \\ 0 &= \left(\frac{R_{rp} + R_{rc}}{s_r} + j\left(X_{rp} + X_{rc}\right)\right)\mathbf{I}_r + j\, X_{mp}\,\mathbf{I}_{sp} - j\, X_{mc}\,\mathbf{I}_{sc}{}^{*} \\ \frac{\mathbf{V}_{sc}}{s_c} &= \left(\frac{R_{sp}}{s_c} + j\, X_{sc}\right)\mathbf{I}_{sc} - j\, X_{mc}\,\mathbf{I}_r{}^{*} \\ T_{ep} &= 3\, p_p\, L_{mp}\, imag\left(\mathbf{I}_{sp}\,\mathbf{I}_{rp}{}^{*}\right) = 3\, p_p\, L_{mp}\, imag\left(\mathbf{I}_{sp}\,\mathbf{I}_r{}^{*}\right)\end{aligned} \tag{10}$$

$$T_{ec} = 3\, p_c\ L_{mc}\, imag\left(\mathbf{I}_{sc}\, \mathbf{I}_{rc}^{*}\right) = -3\, p_c\, L_{mc}\, imag\left(\mathbf{I}_{sc}\, \mathbf{I}_{r}\right) \tag{11}$$

where the slips s_r and s_c are introduced and defined as follows:

$$s_r = \frac{\omega_r}{\omega_p} \text{ and } s_c = \frac{\omega_c}{\omega_p} \tag{12}$$

3.1 Core Loss Modelling

The core loses are modelled classically by using resistors in parallel with magnetising branch. In this way the core losses are proportional to the corresponding magnetising (revolving) flux squared. Contrary to the classical model of an induction machine, the rotor core loses have to be introduced as the frequency of the rotor quantities in the BDFTSIG is much higher than in standard induction machines. Since the resistance modelling the core loses is normally found from the no-load test at 50Hz (power system frequency), to take approximately into account the combined frequency dependence of the core losses, they will be adjusted by the factor $s^{1.3}$, where s is the corresponding slip.

The power machine stator always operates at the power system frequency of 50Hz so that no correction to R_{msp} is required for the power machine stator core losses modelling:

$$P_{Fesp} = 3\frac{E_{mp}{}^2}{R_{msp}} \tag{13}$$

In the synchronous mode the rotors of the both machines operate at the same but variable frequency defined by the rotor slippage with respect to the power system frequency (s_r):

$$P_{Ferp} = 3\frac{E_{mp}{}^2}{R_{mrp}/|s_r|^{1.3}}$$

$$P_{Ferc} = 3\frac{E_{mc}{}^2}{R_{mrc}/|s_r|^{1.3}} \tag{14}$$

The control machine stator operates at variable control frequency defined by the s_c so that the corresponding core loses can be found as:

$$P_{Fesc} = 3\frac{E_{mc}{}^2}{R_{msc}/|s_c|^{1.3}} \tag{15}$$

3.2 Rotor Power Balance in the Presence of Core Losses

To preserve correct power balance at the rotor side the rotor core looses can not be directly modelled by introducing the shunt resistances but it must they have to be scaled by the rotor slip.

$$P_{revolving\ field} = T_{ep}\,\omega_p/p_p = P_{Ferp} + P_{Cu\,rp} + P_{mech\,rp}$$

$$= P_{Ferp} + P_{Curp} + T_{ep}\,\omega_r$$

$$T_{ep}\left(\omega_p/p_p - \omega_r\right) = T_{ep}\,\omega_p/p_p\left(\omega_p - p_p\omega_r\right)/\omega_p =$$

$$= s_r\, T_{ep}\,\omega_p/p_p = P_{Ferp} + P_{Curp}$$

$$P_{revolving\ field} = \left(P_{Ferp} + P_{Curp}\right)/s_r \tag{16}$$

Therefore in equivalent schemes with the modelled rotor core losses an equivalent shunt resistance $R_{mrp}{}'$ dependant on the rotor speed has to be introduced (Fig. 2), for example:

$$R_{mrp}{}'(s_r) = s_r\, R_{mrp}/|s_r|^{1.3} \tag{17}$$

Eq. 16 can be viewed as a generalisation of the traditional steady state model which does not take into account the rotor power losses and where $P_{revolvingfield} = P_{Curp}/s_r$. It is worth noting that the actual rotor core losses should be still calculated as in Eqs. 13-15. The difference between the power developed on the modified resistance $R_{mrp}{}'(s_r)$ and the rotor core loss power is a relatively small amount of the rotor mechanical power produced by the electromagnetic torque component created due to the presence of the rotor core losses. The existence of this torque component was experimentally confirmed in no load tests with open rotor circuits and with stator windings energised at the nominal voltage of 240V. In the tests a small torque component estimated at 2-3 Nm was present created only due to the existence of the rotor core loses.

3.3 Electromagnetic Torque in the Presence of Core Losses

Torque equations (Eqs. 11) should be also modified in the presence of the core losses. No longer the stator and rotor currents I_{sp}, I_{rp} or I_{sc}, I_{rc} should be used for the calculation as in Eq. 11 but the currents $I_{sp}{}'$, $I_{rp}{}'$ or $I_{sc}{}'$, $I_{rc}{}'$ which now mutually interact between the stator and rotor circuits as can be seen in the modified equivalent scheme in Fig. 2.

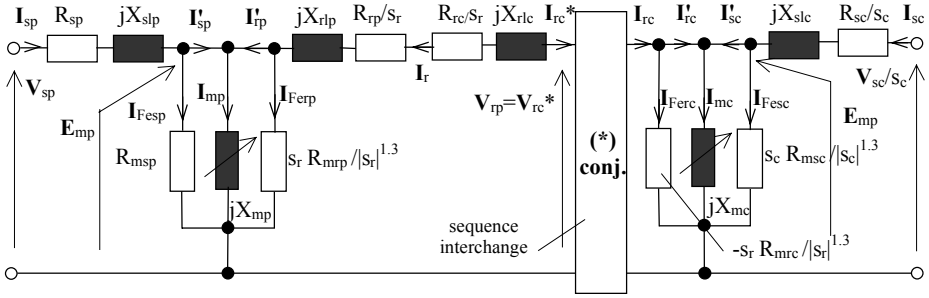

Figure 2. Equivalent steady-state scheme for the BDFTSIG with included and iron magnetic saturation and core loses

$$T_{ep} = 3\, p_p\, L_{mp}\, imag\left(\mathbf{I}_{sp}{}' \, \mathbf{I}_{rp}{}'^{*} \right)$$

$$T_{ec} = 3\, p_c\, L_{mc}\, imag\left(\mathbf{I}_{sc}{}' \, \mathbf{I}_{rc}{}'^{*} \right) \qquad (18)$$

In this way power balance is fully satisfied what has been checked in simulations.

3.4 Magnetic Saturation Modelling

As the control machine is used for regulating the active and reactive power flows through the power machine it does not work in the constant flux mode. Consequently the saturation effect of the iron core can be significant especially when the control machine is heavily excited forcing the power machine to generate reactive power (capacitive power factor). Thus, to obtain a reasonable agreement between the theoretical model and experimental results, the saturation effect also has to be modelled. For our steady state model the inverse curve describing $I_m=f(\lambda_m)$ is necessary so that the following prototype curve is used for the inverse magnetising curve modelling:

$$I_m = c\,(a\,\psi_m + (1-a)\,\psi_m{}^{b}) \qquad (19)$$

3.5 Friction and Ventilation Torque

The torque related to mechanical loses T_{fv} is modelled simplistically as a linear function of the rotor speed. Its value is found to be 6Nm at 1500 rpm so that:

$$T_{fv} = f(\omega) = T_{fvb}\frac{\omega_r}{\omega_b} = 6\frac{\omega_r}{157} = 0.0382\,\omega_r \qquad (20)$$

4. PERFORMANCE STUDY

The steady state performance of the BDFTSIG system is evaluated in the speed range from 600 rpm to 900 rpm for constant active power generated through the power machine of P_{sp}=-20kW for several power factors of the power machine of $\cos\varphi_{sp}$=0.8, 0.9 ind., 1 and 0.9 cap.. The power machine voltage is 240V/50Hz. In order to find the magnetising curve $\lambda_m=f(I_m)$ no load test was performed on the power machine and the results are shown in Table 1. These results are used to fit the inverse magnetising curve model (Eq.) $I_m=f(\lambda_m)$ curve-model by using the Curve Expert software, Version 1.3. It has found that the following curve parameters give the best fit: a=0.51, b=6.52, c=26.4 as shown in Fig.3. The parameters shown in Table 2 used in the performance evaluation and they correspond to the parameters of the machines used in the experimental set-up (two nearly identical IM of 20kW/1500rpm).

The simulation results shown in Fig. 4 depict how major quantities of the BDFTSIG are varying with the rotor operational speed. From these results it is possible to see that the required control voltage (Figs. 4a) and control winding VA rating (4c) depend almost linearly on the rotor speed (i.e. on the control frequency). The lowest values of the control voltage are found nearly at the rotor speed corresponding to the zero control frequency:

$$\omega_r = \frac{\omega_p}{p_p + p_c} \qquad (22)$$

Table 1. No load test results.

Vs [V]	Im [A]	Xm [Ω]	Lm [mH]	Ψm [Wb]
41.28	1.89	21.84	69.56	0.131465
114.63	4.93	23.25	74.05	0.365064
157.63	6.91	22.80	72.61	0.502006
214.40	10.00	21.44	68.28	0.682803
263.10	15.75	16.70	53.20	0.837898
290.80	20.04	14.51	46.21	0.926115
319.80	28.18	11.35	36.15	1.018471
347.10	39.83	8.72	27.76	1.105414

Table 2. Parameters of the BDFTSIG.

R_s [Ω]	R_s [Ω]	L_{sl} [mH]	L_{rl} [mH]	L_m [mH]	R_{ms} [Ω]	R_{mr} [Ω]	p_p	p_c
0.205	0.205	2.14	2.14	model	308	890	2	2

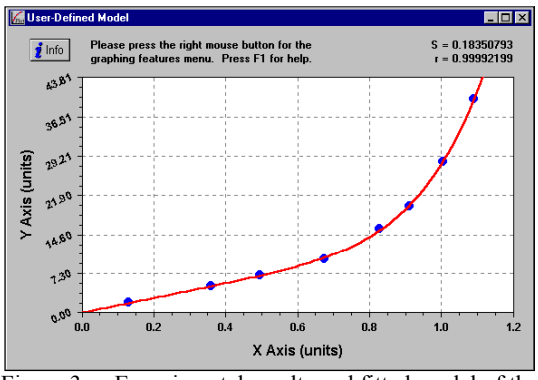

Figure 3. Experimental results and fitted model of the inverse magnetising curve

As the power machine power is kept constant (Figs. 4e), the power machine and control machine stator currents (Fig. 4b) are nearly constant but the control current exhibits a high dependence on the power factor (analogous as in synchronous machines). The lowest control current is required for the inductive power factors (Fig. 4b, approx. 44A for 0.8 ind.), while it is considerable higher if power factor is capacitive (Fig. 4b, approx. 61A for 0.9cap.). Due to nearly constant currents the corresponding power losses are also nearly constant (Fig. 4g). The total electrical power generated by the BDFTSIG is nearly linearly proportional to the rotor speed (Fig. 4e) as the power of the control winding is a linear function of the rotor speed. Below the rotor speed given by Eq. 22 the control machine uses a part of the power generated by the power machine (useless circulation of the power) while above that speed the control winding generates the power which adds up to the power generated by the power machine. Thus the generator efficiency progressively increases as the rotor speed increases

(Fig. 4h). It has the highest value for the inductive power factors since the control current has the lowest value (82%).

The torque in the both machines is approximately constant in the whole speed range (Fig. 4f). It can be noticed that the control machine torque is slightly higher than that of the power machine. As the both machines share common rotor current this is the result of a higher air-gap flux in the control machine. The control machine air-gap flux (Fig. 4i, 0.62-0.89 Wb in terms of rms values) is strongly dependant on the power factor. A relatively high level of the control flux is required for capacitive power factors and thus the control machine iron core is magnetically saturated what is reflected, as we already mentioned, as a very sharp increase in the control current and consequently as a high VA rating of the control machine. The power machine air-gap flux is more stable (Fig. 4i, from 0.56-0.64 Wb) as this machine is connected at stiff power system voltage.

To limit VA rating of the power electronics converter to approx. of ¼ of the power machine rating (to approx. 5kVA) the generator speed range should be restricted to 650 rpm-900 rpm while the power machine power factor must be kept in inductive range (preferably around 0.9). Although possible, it is not economically justified to generate reactive power (capacitive power factors) with the existing control machine design. It would require the control machine/power converter VA ratings of nearly 50% (10kVA for 0.9 cap.) of the power machine VA rating (see Fig 5c) in the speed range of 650rpm or 900rpm. The VA rating for the capacitive power factors can be reduced significantly but the control machine must be redesigned for the flux levels required for such applications to avoid its heavy magnetic saturation.

As the electromagnetic torque of the bot machine are similar the amount of the active materials in the both machines must be nearly the same (same volume). It may be unexpected as we just have shown that the control machine VA rating is much lower than that of the power machine. However the lower VA is the result of a low operational frequency of the control machine (consequently low control voltage) while the control current and flux are even higher then these in the power machine. Therefore it is expected that in realistic BDFTSIG the actual volume of the control machine may need to be slightly bigger than that in the power machine. But it does not mean that in this way we are paying a heavy penalty for avoiding the slip rings and brushes by obtaining a very bulky generator system.

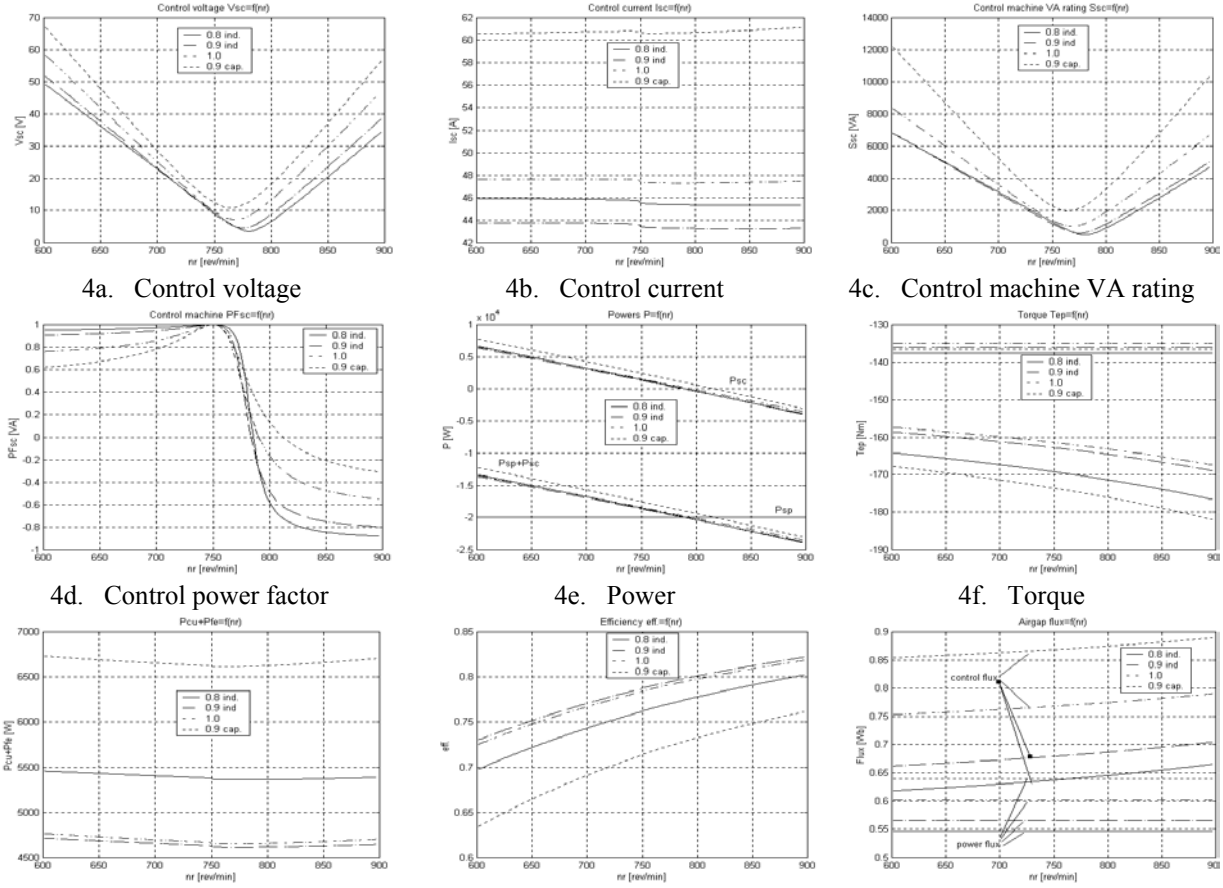

4a. Control voltage 4b. Control current 4c. Control machine VA rating

4d. Control power factor 4e. Power 4f. Torque

4g. Copper+core losses 4h. Efficiency 4i. Air-gap flux (rms)

Fig.4 Simulation results for P_{sp}=-20kW for different power factors in the speed range of 600-900 rpm

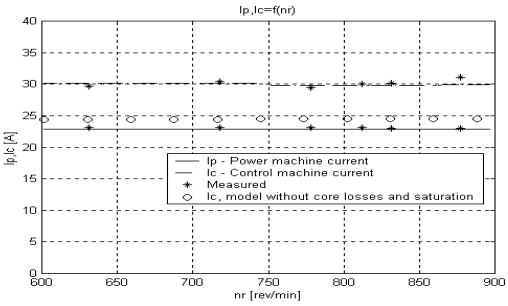

5a. Power and control machine currents

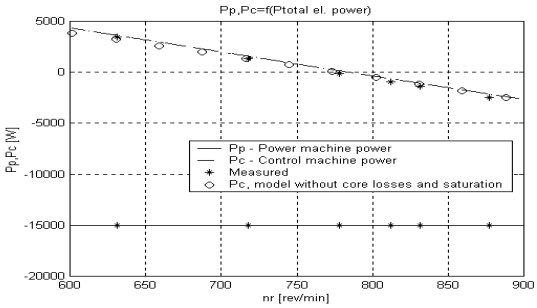

5b. Power and control machine currents

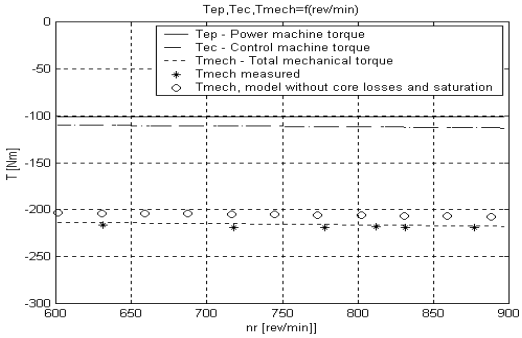

5c. Torque

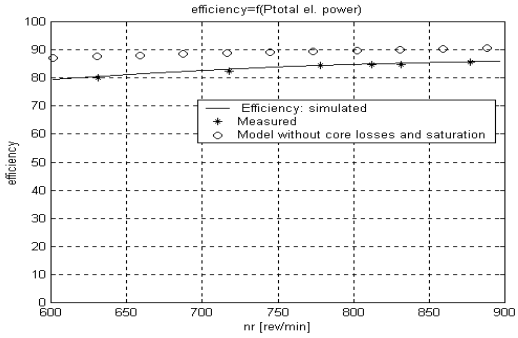

5d. Efficiency

Figure 5. Comparison of the simulation and experimental results for –15kW and 0.9 inductive

The fact is that the both machines are able to produce full nominal torque. Thus in the BDFTSIG we actually doubled the total torque while the base speed is halved (Eq. 22, the same number of poles: $p_p=p_c=2$), i.e. the ratio between the torque and speed is simply redistributed (exactly as a gear box does). Therefore, for the same number of poles of the power and control machines, the BDFTSIG has power rating of a single stator but it behaves as it had twice number of poles. Thus it is expected that the two stators of the BDFTSIG combined should be nearly the same in volume as the stator of an equivalent slip ring standard induction machine of the same power and with the pole number equal p_p+p_c. In our case we have obtained from two nearly identical 20kW/1500rpm induction machines an equivalent of the BDFTSIG of 20kW operating at the base speed of 750 rpm.

Experimental result for P_{sp}=–15kW=const. (due restricted power of the prime mover) and power factor of 0.9 ind. are shown in Fig. 5. These results compare very well with the simulation results what confirms the accuracy of the developed steady state model. Big errors in the prediction of the control current (24A instead 30A), torque and efficiency are noticeable when the core losses and saturation are neglected (results marked by 'o', for unsaturated $L_{mp}=L_{mc}=$ 85mH, and $R_{msp}=R_{mrp}=R_{msc}=R_{mrc}\rightarrow\infty$).

5. CONCLUSION

The paper has presented steady state model of the BDFTSIG that accounts magnetic saturation and core losses. Using the proposed model a performance study of the BDFTSIG has been carried out. It shows that the BDFTSIG efficiency varies between 70%-82% in the speed range from 650 to 900 rpm (depending on the power factor) while the VA rating of the control machine (power electronics converter) is less then a ¼ of the power machine VA rating.

As the BDFTSIG behaves as a robust brushless equivalent of a doubly fed variable speed generator we anticipate that it will be practical for large wind generators.

6. REFERENCES

[1] R. Pena, J.C. Clare, G.M. Asher, "Doubly fed induction generator using back-to-back PWM converters and its application to variable speed wind-energy generation", IEE Proc.-Electr. Power Appl., Vol.143, No.3, 1996, pp231-241

[2] S. Muller, M. Deicke, R.W. De Donncker, "Adjustable Speed Generators for Wind Turbines based on Doubly-fed Induction Machines and 4-quadrant IGBT Converters Linked to the Rotor", IEEE Industry Applications Conference, Vol.4, 2000, pp.2249-2254

[3] B. Hopfensperger, D.J. Atkinson, R.A. Lakin, "Stator flux oriented control of a cascaded doubly-fed induction machine", IEE Proc.-Electr. Power Appl., Vol.146, No.6, 1999, pp597-605

[4] B. Hopfensperger, D.J. Atkinson, R.A. Lakin, "Combined magnetising flux oriented control of the cascaded doubly-fed induction machine", IEE Proc-Electr Power Appl, Vol.148, No.4, 2001, pp354-362

[5] D. Zhou, R. Spee, G.C. Alexander, "Experimental Evaluation of a Rotor Flux Oriented Control Algorithm for Brushless Doubly-Fed Machines", IEEE Trans. on Power Electronics, Vol.12, No.1, 1997, pp.72-78